Supporting Information

On-surface Polymerization on a Semiconducting Oxide: Aryl Halide Coupling Controlled by Surface Hydroxyl Groups on Rutile TiO$_2$(011)

Marek Kolmer, Rafal Zuzak, Amir A. Ahmad Zebari, Szymon Godlewski, Jakub S. Prauzner-Bechcicki, Witold Piskorz, Filip Zasada, Zbigniew Sojka, David Bléger, Stefan Hecht and Marek Szymonski

Table of contents:

1. Experimental methods

The experiments were carried out in an ultra-high vacuum (UHV) system with the base pressure in the 5×10^{-11} mbar range. Single crystal rutile TiO_2(011)-(2×1) surfaces (MTI corporation) were prepared by several cycles of Ar^+ sputtering performed at room temperature (incident angle 45°, ion energy 0.6 keV, 10 min) and subsequent 10 min annealing at 1050 K as monitored by an infrared pyrometer. The quality of the reduced TiO_2(011)-(2×1) substrates was then checked by the low-energy electron diffraction (LEED) and scanning tunneling microscopy (STM) imaging. For preparation of the hydroxylated surfaces the atomic hydrogen, provided by a home-built hydrogen cracker, was dosed to the samples kept at room temperature. The surface hydroxyls were also removed from the hydroxylated samples by their annealing at 370 K in oxygen 10^{-7} mbar partial pressure. The diiodoterfluorene (**DITF**) and dibromoterfluorene (**DBTF**) molecules were deposited from a three-cell Kentax effusion cell with the crucible kept at 495 K and 490 K , respectively. For all experiments the molecular flux was calibrated with use of a quartz microbalance. In all cases excluding quadrupole mass spectrometry (QMS) experiments the nominal coverage of precursor molecules calculated from STM images was 0.30 ± 0.05 monolayer (ML). Here we define 1 ML of precursor molecules by the density of close-packed **DITF** molecules in the adsorption geometry presented in Fig. 2a and 2c of the manuscript, *i.e.* 4.04×10^{13} cm^{-2}. After the precursor deposition the samples were transferred immediately (<5 min) to the cryostat of the low-temperature STM (LT-STM), where they were cooled down to 77 K (liquid nitrogen). All STM images presented in this work were acquired with use of the LT- STM (Omicron GmbH) operating at 77 K. QMS experiments were performed with application of the Hidden Hal 301 mass spectrometer located about 4 cm from the surface of the sample. During the QMS analysis the samples were heated with a linear rate of about 3.4 K/s as checked by the K-type thermocouple and the pyrometer (for temperatures lower than 420 K temperature readout was interpolated). Sample heating was accomplished using a silicon wafer mounted beneath the sample and directly heated by alternating current.

2. Synthesis of the diiodoterfluorene (DITF) monomer

Diiodoterfluorene (**DITF**) was synthesized from terfluorene (**TF**), prepared according to our published route,[1] by iodination using N-iodosuccinimide (NIS)[2] as outlined in Fig. S1.
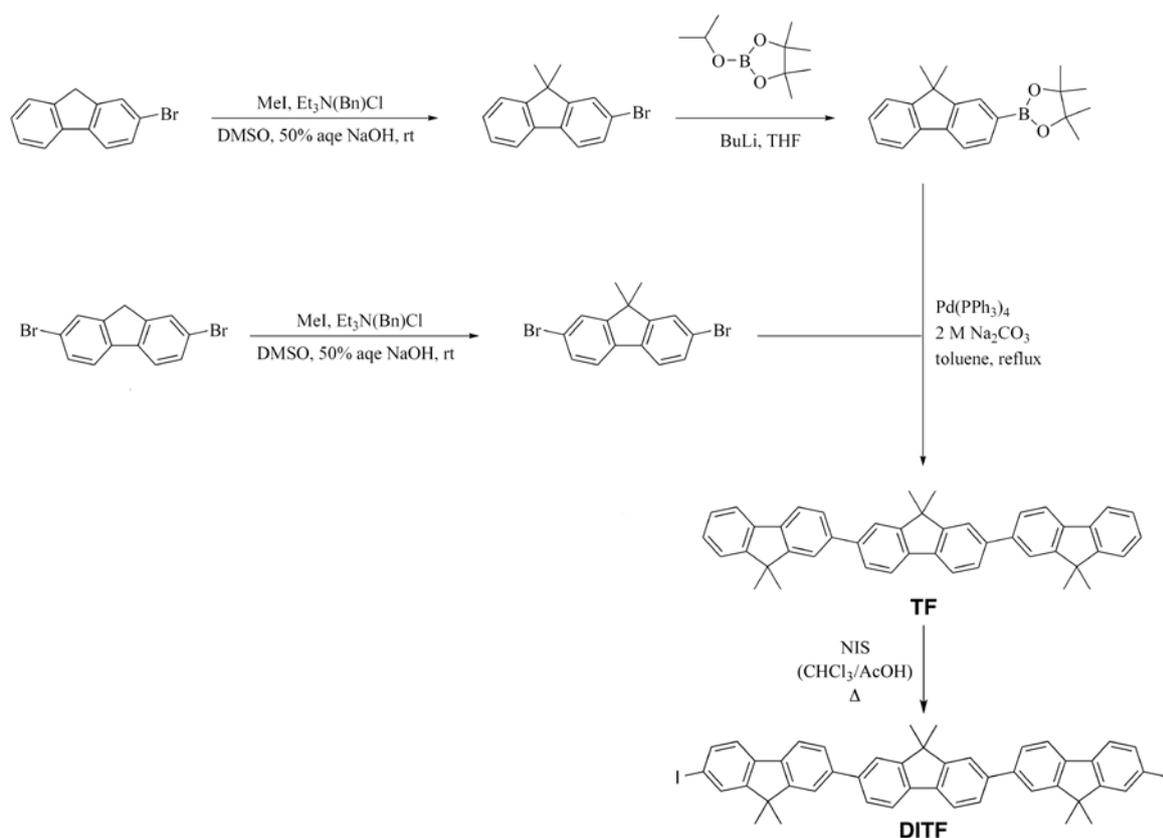
Fig. S1 Synthesis of diiodoterfluorene monomer (**DITF**).

To a solution of **TF** (250 mg, 0.43 mmol) in 15 mL of CHCl$_3$/AcOH (2:1) was added NIS (485 mg, 2.16 mmol). The reaction mixture was refluxed for 18 h, washed with water, and concentrated under vacuum. The product was precipitated from hexanes/methylene chloride mixtures and further purified by preparative gel permeation chromatography (GPC) to separate the product from the mono- and tri-iodinated compounds yielding **DITF** as white solid (50 mg of pure **DITF** after prep. GPC of 200 mg of the product mixture).

^{1}H-NMR (300 MHz, CDCl$_3$): δ(ppm) = 7.88–7.85 (d, 2H), 7.83–7.73 (m, 4H), 7.75–7.67 (m, 10H), 7.55–7.52 (d, 2H), 1.67 (s, 6H), 1.58 (s, 12H). ^{13}C-NMR (75 MHz, CDCl$_3$): δ(ppm) = 156.1, 154.6, 141.5, 138.6, 138.2, 136.1, 132.1, 126.5, 126.4, 121.8, 121.4, 120.4, 47.2, 47.1, 27.4, 27.1; HRMS-ESI: m/z = 830.1003 (calcd for [M$^{+\bullet}$], 830.0906).

3. Determination of the optimal experimental conditions: polymerization reaction byproducts

In order to follow the behavior of polymerization reaction byproducts as a function of the substrate temperature we combined STM measurements with an *in-situ* quadrupole mass spectrometer (QMS) analysis. Firstly, we deposited a full monolayer of **DITF** on *5%H*-TiO_2(011) kept at RT. The evaporation of the complete layer was chosen to achieve the sufficient number of reacting molecules that would enable detection of the reaction byproducts in QMS. Afterwards, we subsequently recorded the QMS signals attributed to the HI and I_2 molecules (m/z=128 and m/z=254) during the controlled sample heating up to 400 °C (Fig. S2). The QMS signals of both analyzed species show the appearance of the pronounced peaks starting at around 260 °C (dashed black line). Complementary STM measurements show that during such thermal treatment an initially unordered layer of precursors was transferred into oligomers (Fig. S3). Presented QMS analysis explains the reduced number, or even complete disappearance of surface defects related to the polymerization byproducts for the **DITF** precursors deposited at 260 °C (see Fig. 3b in the manuscript). At this temperature the iodine atoms are effectively desorbed from the surface in the form of the HI and I_2 molecules. In contrary to that, after **DBTF** deposition on *5%H*-TiO_2(011) at 260 °C, polymerization byproducts stay on the surface. The corresponding STM image in Fig. S4a clearly shows oligomers, as well as, bromine-related defects present on the surface. Additionally similar QMS experiment for **DBTF** has not yielded any substantial signal coming from the reaction byproducts (Br, HBr and Br_2) for temperatures up to 300 °C. Oligomer formation on *5%H*-TiO_2(011) at 260 °C without additional reaction byproducts observed on the surface is the reason to use **DITF** instead of **DBTF** in the reported experiments. Finally, the polymerization reaction of the **DITF** precursors takes place also at lower temperatures than 260 °C, *i.e.* at 200 °C, but in this case the reaction byproducts in the form of iodine atoms (most probably adsorbed on surface hydroxyl groups) are present on the surface (Fig. S4b). Note that this result is in agreement with the QMS experiment as well.
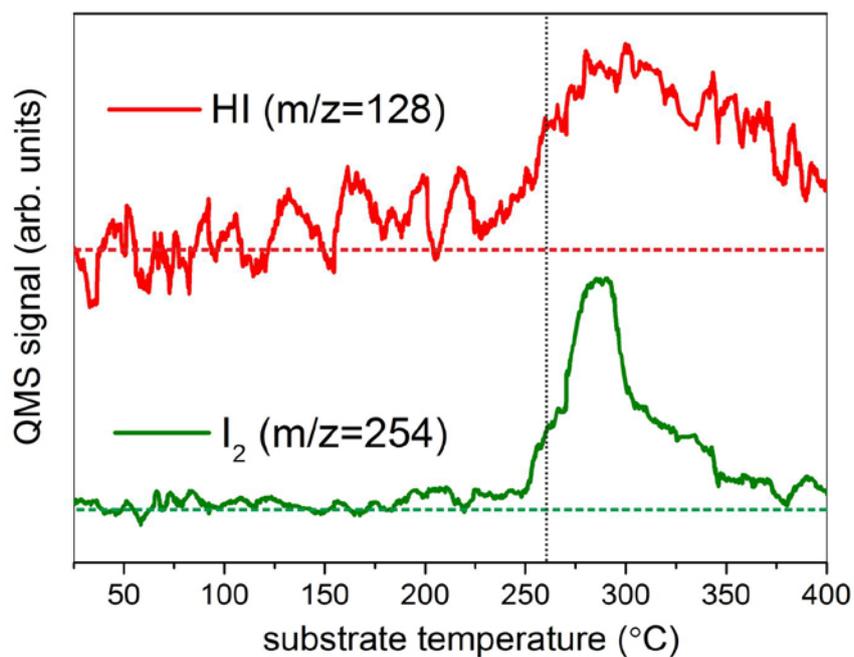
Fig. S2. QMS spectra for m/z=128 (HI) and m/z=254 (I_2) obtained during controlled heating of the *5%H*-TiO_2(011) covered by one monolayer of **DITF** molecules deposited at RT.
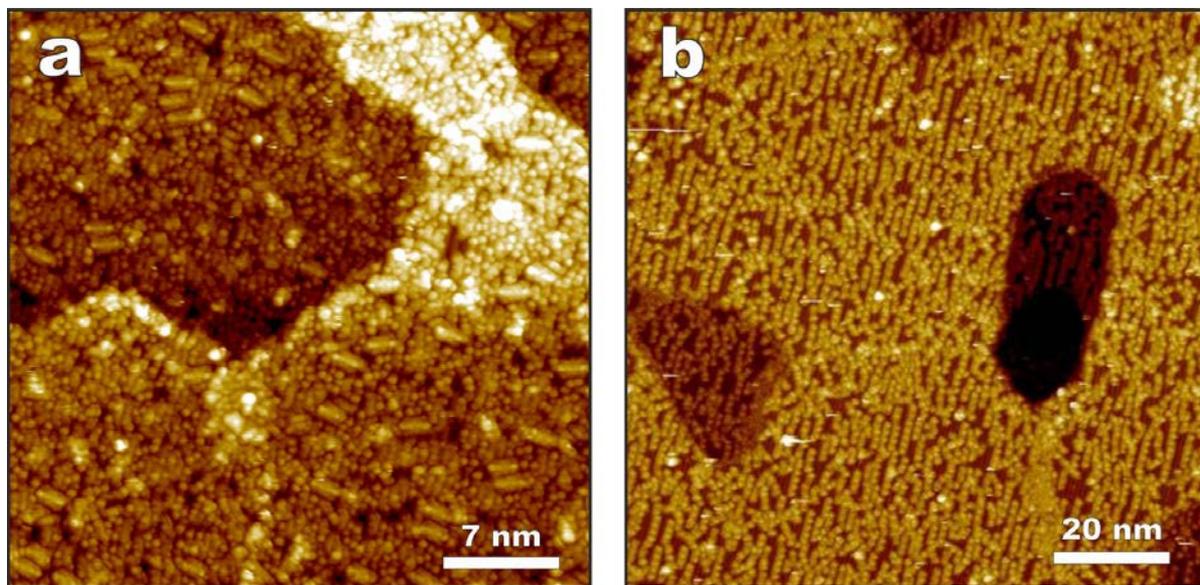
Fig. S3. STM images of **DITF** molecules deposited on the *5%H*-TiO_2(011) substrate kept at RT obtained (a) before and (b) after controlled heating of the sample to 350 °C. The STM parameters are +2 V, 5 pA in (a) and +1.2 V, 5 pA in (b).
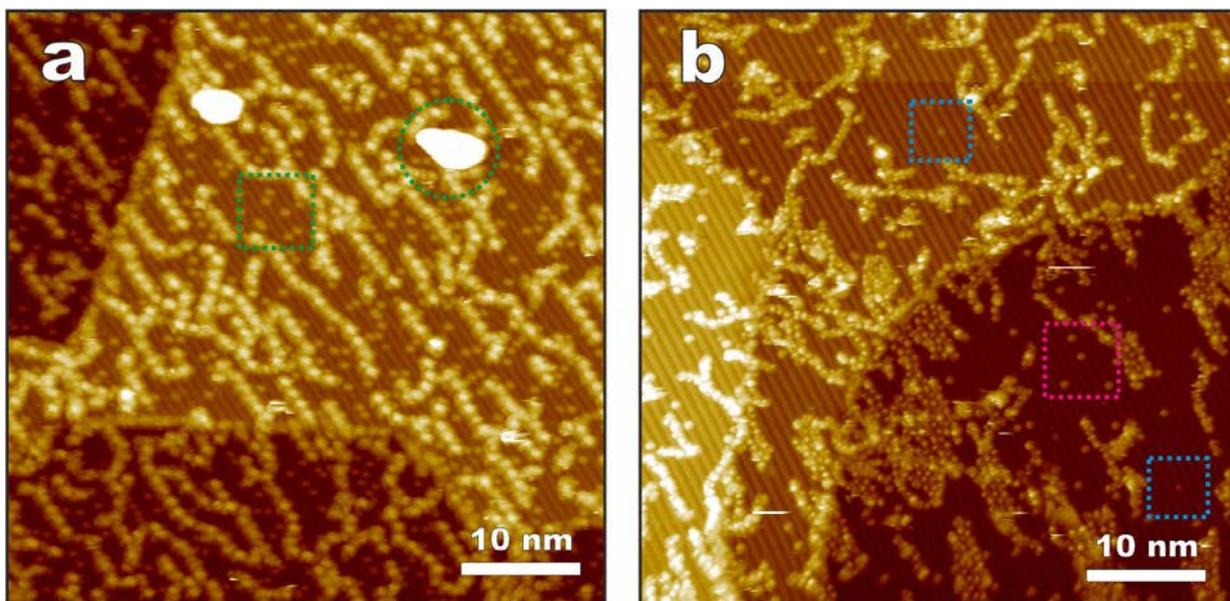
Fig. S4 (a) STM image of **DBTF** deposited on the *5%H*-TiO$_2$(011) substrate kept at 260 °C. Green circle and square point to Br-related defects on the surface: clusters (circle) and single bromine atoms adsorbed on the surface (square). Please note that similar defects were also observed after polymerization of the 10,10'-dibromo-9,9'-bianthryl (**DBBA**) molecules on the TiO$_2$(011) surface (see reference 11 in the manuscript) (b) STM image of **DITF** deposited on the *5%H*-TiO$_2$(011) substrate kept at 200 °C. Purple square marks iodine atoms adsorbed on the surface. Blue squares mark surface hydroxyl groups, which exhibit lower altitude than the iodine atoms. For both images the STM parameters are +2 V, 10 pA. To compare with **DITF** deposited on *5%H*-TiO$_2$(011) at 260 °C please refer to Fig. 3b in the manuscript.

4. **Additional STM images of diiodoterfluorene (DITF) molecules deposited on differently prepared rutile TiO$_2$(011) substrates**
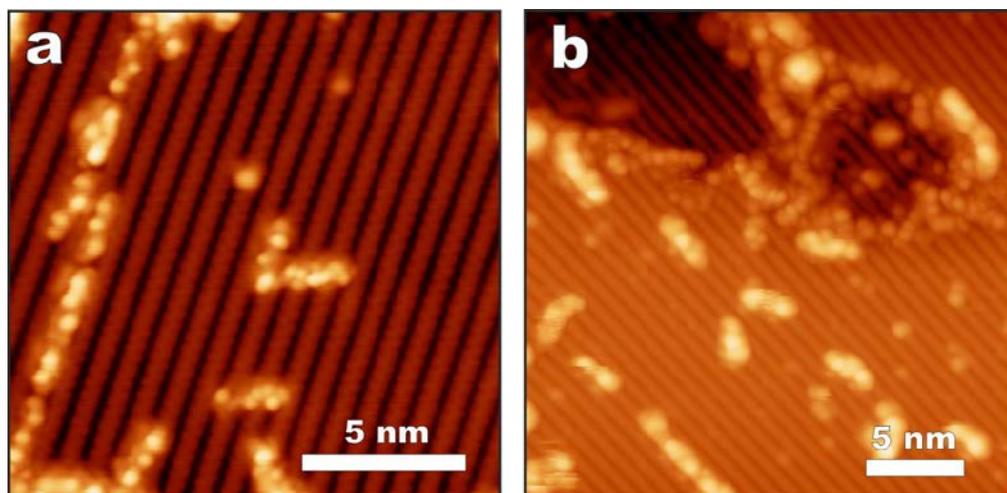
Fig. S5 (a) STM image of **DITF** molecules deposited on reduced *r*-TiO$_2$(011) kept at 260 °C (15×15 nm^2, +2 V, 10 pA). (b) STM image of **DITF** molecules deposited on oxidized *o*-TiO$_2$(011) kept at 260 °C (25×25 nm^2, +2 V, 10 pA). The polymerization reaction does not occur in both cases. Note that due to the preparation procedure of *o*-TiO$_2$(011) additional surface defects, i.e. adsorbed water molecules are present, and in this case the fraction of the **DITF** molecules found directly on terraces is higher.
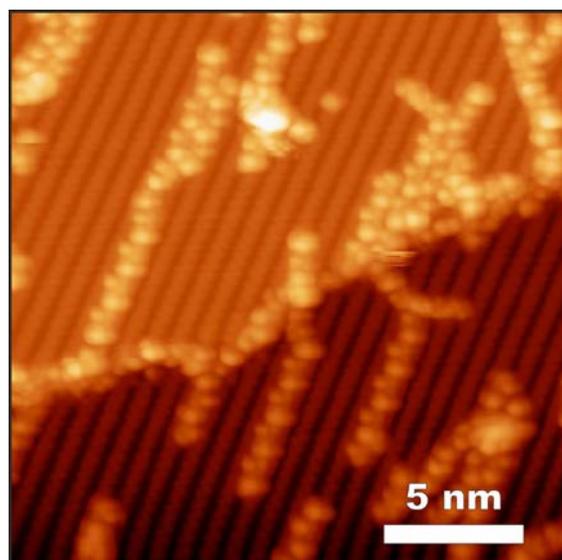
Fig. S6 High resolution STM image of **DITF** molecules deposited on moderately hydroxylated *5%H*-TiO$_2$(011) kept at 260 °C (20×20 nm^2, +2 V, 10 pA). Polyfluorene chains covering two reconstructed terraces of TiO$_2$(011)-(2×1) are clearly seen. Note that almost defect-free TiO$_2$(011)-(2×1) surface regions between the oligomers are found.

7
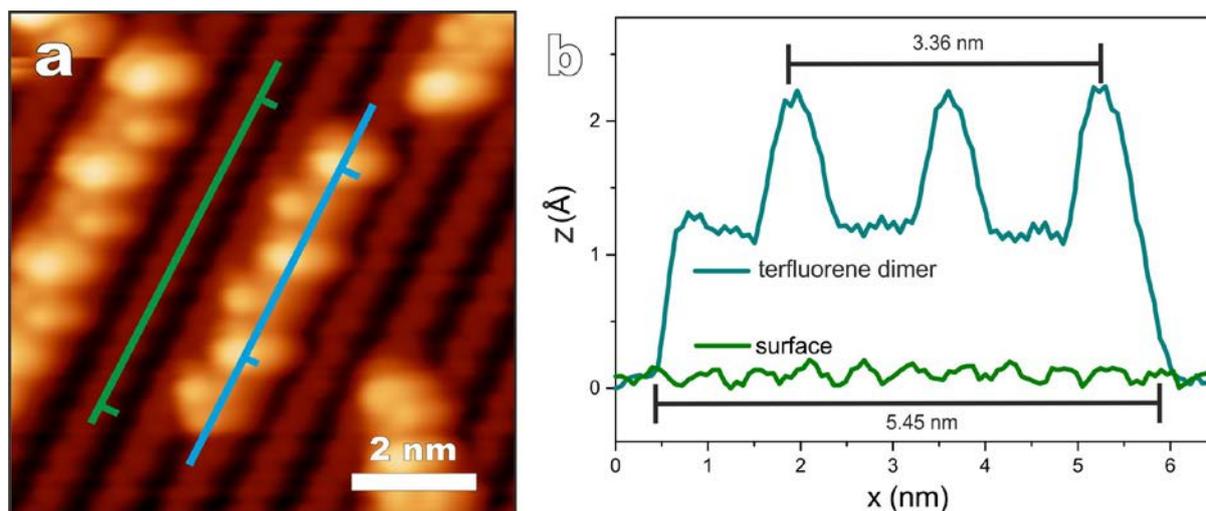
Fig. S7 (a) High resolution STM image of terfluorene dimer with lines corresponding to STM image cross sections presented in (b). STM parameters are +2 V, 10 pA. (b) STM cross sections of the $TiO_2(011)$-(2×1) surface along the [01-1] direction (green) and the terfluorene dimer (blue). Measured 3.36 nm distance between the pronounced peaks on the molecule represents the length of four fluorene units, what corresponds to 0.84 nm per single fluorene unit. This result is in perfect agreement with the expected 0.845 nm value for covalently coupled monomers. The measurement was calibrated by the $TiO_2(011)$-(2×1) surface periodicity along the [01-1] direction (0.545 nm). Distance of 5.45 nm corresponds in this case to the length of ten surface unit cells.

8

5. Calculation details

For all calculations the first principles DFT theory implemented in the Vienna Ab-initio Simulations Package (VASP) was chosen.[3] The projector augmented plane wave (PAW) method[4] for describing electron-ion interactions together with PW91 GGA exchange-correlation functional parameterized by Perdew et al.[5] was employed. Additionally, to account for dispersion forces the semi-empirical Grimme[6] correction of the DFT method (DFT-D) was included. The Brillouin zone sampling at Γ point with the cut-off energy of 350 eV and the Gaussian smearing with σ parameter set to 0.05 eV were used. The energy convergence criterion for solving the Kohn-Sham equations was set to 10^{-5} eV. Geometry optimization was performed until the changes in the forces acting on the ions were smaller than 10^{-4} eV/Å per atom.

The slab models of (011) rutile surface were constructed by cleaving the crystal along the (011) plane with the "brookite (001)-like" termination proposed independently by Torrelles et al.[7] and Gong et al.[8] This termination not only reproduces correctly STM pattern, but also has the lowest surface energy among already reported structures, and can be formed from bulk-like termination by only local displacements of atoms (mass transport is not required). For all calculations we used the (4 × 3) supercell slab with stoichiometry $Ti_{160}O_{320}$, and dimension of a = 18.378 Å, b = 32.787 Å, and c = 32.00 Å, along the [100], [0-11], and [011] directions of the rutile structure, respectively. The oxide thickness was chosen as 11.77 Å (nine atomic layers) and periodically multiplied layers were separated with the wide vacuum region of ~20 Å, large enough to accommodate the **DITF** molecule and to avoid mutual interactions. In each calculations the adsorbed molecules/species and the six topmost layers of surface ions were fully optimized whereas the rest of the oxide ions were fixed in their positions. The **DITF** molecule adsorption optimized within described unit cell (Fig. S8) was then used to simulate the STM image (Fig. 2d in the manuscript). Optimal orientation of the adsorbed molecule was found along the [0-11] rows of two-fold oxygen atoms and ~2.7 Å above them (Fig. S8). Molecule preserves its nearly linear gas-phase geometry, with slight attraction of iodine terminal atoms toward surface. Adsorption energy is rather small (-0.72 eV per molecule) and results from the molecule–substrate attractive interactions (-2.11 eV) counterbalanced by the **DITF** molecule deformation (+1.39 eV). Most of the

interaction energy is covered by the dispersion forces (~75 %), what stems from the large area of substrate/admolecule contact.

The nudged elastic band method (NEB),[9] with a total of six to ten images, was used to calculate energy barriers for proton transfer from TiO_2 to **DITF** molecule, and for modeling of the **DITF** coupling (C-C bond formation). The coupling process was studied with employment of: (1) two protonated molecules (**DITF**H$^+$-**DITF**H$^+$), (2) two intact molecules (**DITF-DITF**), (3) intact and protonated molecules (**DITF-DITF**H$^+$).
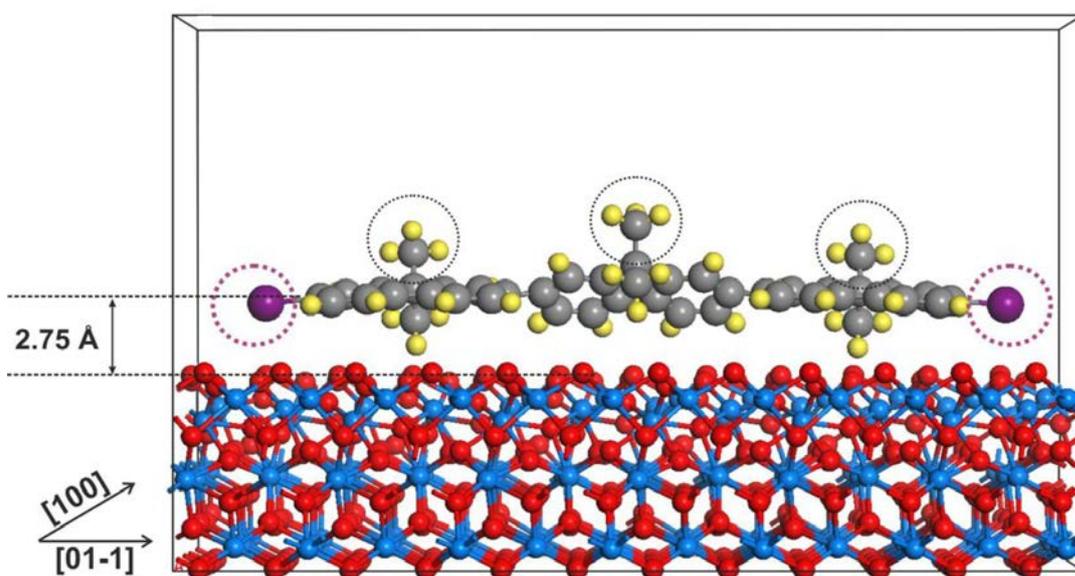
Fig. S8 Optimal position of **DITF** over the rutile TiO_2(011) surface. The protruding methyl groups and the iodine atoms are encircled. These parts of the admolecule contribute mostly to STM signal.

The STM images of **DITF** and **TF** molecules adsorbed on TiO_2(011) surface were simulated as topographies of constant local density of states, with the constant current (I = 2 pA) mode applied as in the STM experiments and bias voltage of +2 V (empty states) via the Tersoff-Hamann level of theory.[10] The five lobe structure and the overall length of the experimental image (Fig. S9a) is well reproduced in the simulated STM image obtained for the **DITF** molecule with the two terminal iodine atoms (Fig. S9b), in contrast to shorter three lobe pattern obtained for the **TF** molecule without the terminal iodine atoms (Fig. S9c).
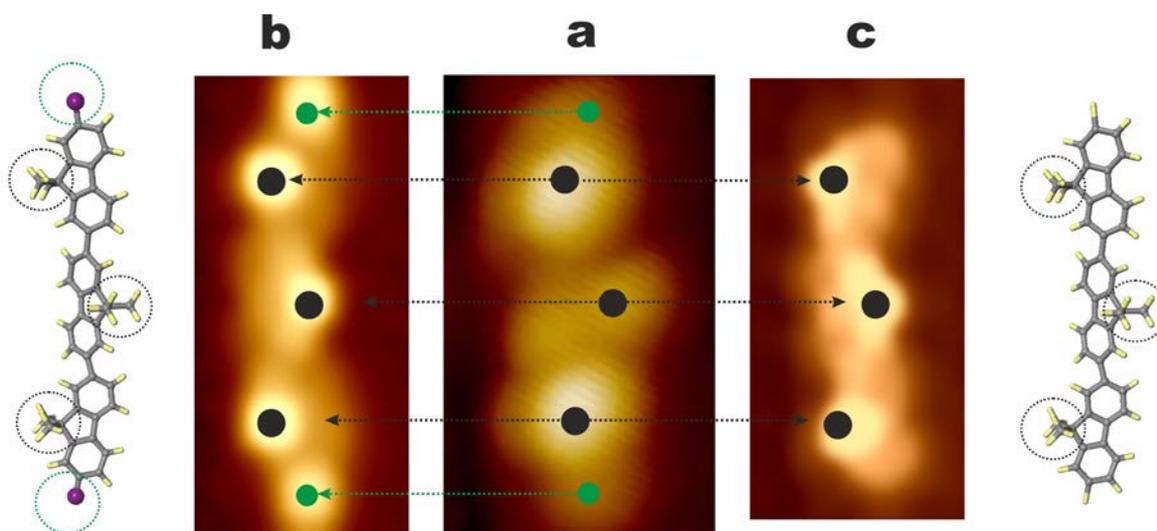
Fig. S9 (a) High resolution experimental STM image of a single **DITF** molecule on TiO$_2$(011) surface. Tersoff-Hamann simulated images of a **DITF** (b) and **TF** (c) molecules with the corresponding molecular models.

6. **References**

[1] L. Lafferentz, F.Ample, H. Yu, S. Hecht, C. Joachim, L. Grill, *Science*, 2009, **323**, 1193-1197.

[2] V.K. Chaikovskii, V.I. Skorokhodov, V.D. Filimonov, *Russ. J. Org. Chem.*, 2001, **37**, 1503-1504.

[3] J. Hafner, *J. Comput. Chem.*, 2008**, 29**, 2044-2078.

[4] P.E. Blochl, *Phys. Rev. B*, 1994**, 50**, 17953-17979.

[5] J. P. Perdew, Y. Wang, *Phys. Rev. B*, 1992, **45**, 13244.

[6] S. Grimme, *J. Comput. Chem.*, 2006**, 27**, 1787-1799.

[7] X. Torrelles, G. Cabailh, R. Lindsay, O. Bikondoa, J. Roy, J. Zegenhagen, G. Teobaldi, W.A. Hofer, G. Thornton, *Phys. Rev. Lett.*, 2008**, 101**, 185501.

[8] X.Q. Gong, N. Khorshidi, A. Stierle, V. Vonk, C. Ellinger, H. Dosch, H.Z. Cheng, A. Selloni, Y.B.He, O. Dulub, U. Diebold, *Surf. Scie.*, 2009**, 603**, 138-144.

[9] G. Henkelman, H. Jonsson, *J. Chem. Phys.*, 2000, **113**, 9978.

[10] J. Tersoff, D.R. Hamann, *Phys. Rev. B*, 1985**, 31**, *805*-813.